PRAMANA
— journal of
physics

Vol. 52, No. 6
June 1999
pp. 561–577

Statistical dynamics at critical bifurcations in Duffing–van der Pol oscillator

V CHINNATHAMBI and S RAJASEKAR*
Department of Physics, AKGS Arts College, Srivaikundam 628 619, India
*Department of Physics, Manonmaniam Sundaranar University, Abishekapatti, Tirunelveli 627 012, India

MS received 15 September 1998; revised 7 April 1999

Abstract. We study the characteristic features of certain statistical quantities near critical bifurcations such as onset of chaos, sudden widening and band-merging of chaotic attractor and intermittency in a periodically driven Duffing–van der Pol oscillator. At the onset of chaos the variance of local expansion rate is found to exhibit a self-similar pattern. For all chaotic attractors the variance $\sigma_n(q)$ of fluctuations of coarse-grained local expansion rates of nearby orbits has a single peak. However, multiple peaks are found just before and just after the critical bifurcations. On the other hand, $\sigma_n(q)$ associated with the coarse-grained state variable is zero far from the bifurcations. The height of the peak of $\sigma_n(q)$ is found to increase as the control parameter approached the bifurcation point. It is maximum at the bifurcation point. Power-law variation of maximal Lyapunov exponent and the mean value of the state variable x is observed near sudden widening and intermittency bifurcations while linear variation is seen near band-merging bifurcation. The standard deviation of local Lyapunov exponent $\Lambda(X, L)$ and the local mean value $\overline{x}(L)$ of the coordinate x calculated after every L time steps are found to approach zero in the limit $L \to \infty$ as $L^{-\beta}$. β is sensitive to the values of control parameters. Further weak and strong chaos are characterized using the probability distribution of a k-step difference quantity $\Delta x_k = x_{i+k} - x_i$.

Keywords. Duffing–van der Pol oscillator; coarse-grained local expansion rates; coarse-grained state variable; weak and strong chaos.

PACS Nos 05.45

1. Introduction

During the last decade or so remarkable progress has been made in exploring the complexity of nonlinear systems, where the presence of chaos and other related phenomena have been extensively investigated [1–5]. Particularly, routes to chaos, characterization of periodic and chaotic motion, controlling and synchronization of chaos etc have been studied in detail. In dissipative chaotic systems drastic change in the structure of chaotic attractor occurs at certain discrete values of control parameters. This includes sudden widening and destruction of a chaotic attractor, band-merging and intermittency. At these bifurcations large fluctuations of coarse-grained statistical measures occur.

Different types of variation of maximal Lyapunov exponent λ have been found near various bifurcations. For one-dimensional maps Huberman and Rudnick [6] have derived a universal scaling power-law for the change of Lyapunov exponent as a function of a control parameter near the period doubling accumulation point. Their scaling law was verified in an experimental system [7]. Linear variation of λ is observed for band-merging crisis and strange nonchaotic to chaotic route [8]. For sudden widening and intermittency crises λ is found to obey power-law scaling [9]. Prasad *et al* [10] studied behaviour of λ for torus to strange nonchaotic transition. On the torus λ is found to vary smoothly while irregular variation is found in strange nonchaotic phase.

Several investigations on certain statistical quantities were performed earlier but mostly for randomly chosen values of control parameters. For example, Voglis and Contopoulos showed that the distribution of local expansion rate is invariant [11]. Variations of local Lyapunov exponent ($\Lambda(X, L)$) about the mean Lyapunov exponent is found to approach zero as $L \to \infty$ [12]. Amitrano and Berry [13] analysed the probability distribution of local Lyapunov exponent for various orbits in Hamiltonian systems. Prasad *et al* [14] observed sharp change in the Lyapunov exponent and large fluctuations of local Lyapunov exponent at the creation of strange nonchaotic attractor.

In the present paper we consider the periodically driven Duffing–van der Pol (DVP) equation

$$\ddot{x} + p\dot{x}(1 - x^2) + \alpha x + \beta x^3 = f \cos \omega t \tag{1}$$

and study

(i) the variance of local expansion rate at the onset of chaos,

(ii) characterization of chaotic attractors at bifurcations using the variance $\sigma_n(q)$ of coarse-grained local expansion rates of nearby orbits,

(iii) characterization of fluctuations of short-time average of the state variable x,

(iv) variation of the scaling exponent β associated with the standard deviation of local Lyapunov exponent $\Lambda(X, L)$ and local mean value $\overline{x}(L)$ calculated after L time steps near critical bifurcations,

(v) variation of maximal Lyapunov exponent and the mean value of the state variable x near critical bifurcations and

(vi) characterization of weak and strong chaos.

The motivation for our interest in this system is that it has wide range of applications in physics and biology. Equation (1) is an alternative form of Bonhoeffer–van der Pol oscillator [15], driven magnetic oscillator [16] and also describes the dynamics of charge density in the plasma of a rf gas discharge. It exhibits well developed chaos in the parameter space [16–18].

2. Dynamic behaviours of critical 2^∞ attractor

In this section, we numerically study the features of the coarse-grained local expansion rate of critical 2^∞ attractor of the system (1). In eq. (1) we fix the parameters values as $p = 0.4$,

$\alpha = -1.0, \beta = 5.0$ and $\omega = 1$. When the control parameter f is varied we found cascade of period doubling bifurcation accumulating at the critical point $f = f_\infty = 0.10976680...$ at which the attractor becomes a critical 2^∞ attractor.

Let $\{X_n\}, n = 1, 2, ...$ be a chaotic orbit generated by a two-dimensional Poincaré map of the DVP oscillator and define the coarse-grained expansion rates [19]

$$\Lambda_n(X_1) = \frac{1}{n} \sum_{m=1}^{n} \lambda(X_m) = S_n(X_1)/n, \tag{2}$$

where $\lambda(X_m)$ is the local expansion rate of nearby orbits at X_m along the unstable manifold. The sum $S_n(X_1)$ fluctuates with n, depending upon the initial value X_1. The rate $\Lambda_n(X_1)$ takes different values between a maximum value $\Lambda_{n,\max}$ and minimum value $\Lambda_{n,\min}$ depending on the initial condition X_1. As $n \to \infty$, $\Lambda_n(X_1)$ converge to a positive Lyapunov exponent Λ^∞ . We consider the variance

$$\langle [S_n(X) - n\Lambda^\infty]^2 \rangle = \frac{1}{N} \sum_{m=1}^{N} [S_n(X_m) - n\Lambda^\infty]^2. \tag{3}$$

We have numerically calculated $\lambda(X_m)$ employing Wolf *et al* [20] algorithm. The Wolf *et al* algorithm has been often used to compute Lyapunov exponents. We computed Lyapunov exponents employing the algorithm for polynomial [15, 21, 22] and nonpolynomial [23] evolution equations, Henon map [24] for periodic, quasiperiodic, chaotic attractors and also at the period doubling bifurcation points. The numerical values of Lyapunov exponents are in good agreement with the actual dynamics. For a chaotic attractor $S_n(X_1)$ grows with n for larger n. However, for the critical 2^∞ attractor at $f = f_\infty$, Λ^∞ is zero indicating that the attractor has no mixing. At $f = f_\infty$ the variance has an interesting behaviour. Figure 1 shows the variance as a function of $\log_2 n$, where N is taken as 3000 in eq. (3). $S_n(X_1)$ grows at most less than linear with n. The plot shows a fascinating temporal structure. The mth block lying between $\log_2 n = m$ and $\log_2 n = m + 1, m = 0, 1, 2, ...$ consists of 2^{m+1} points. As m increases the block exhibits a self-similar pattern.

Self-similar pattern is also seen in the time series of the exponent

$$\beta_n(X_1) = S_n(X_1)/\ln(n). \tag{4}$$

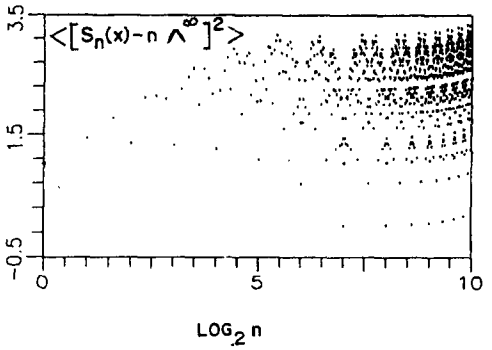

Figure 1. Variance $\langle [S_n(X) - n\Lambda^\infty]^2 \rangle$ versus $\log_2 n$ for the DVP oscillator eq. (1), where $f = f_\infty \approx 0.10976680$ (onset of chaos) and $N = 3000$.

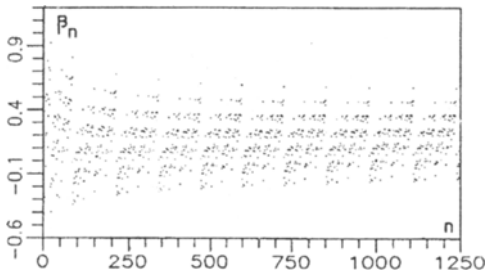

Figure 2. β_n is plotted against n for the chaotic attractor at $f_\infty = 0.10976680$.

$\beta_n(X_1)$ versus n is plotted in figure 2. $\beta_n(X_1)$ does not converge to any constant value nor diverge in the limit $n \to \infty$ but fluctuations continues infinitely. The time series of $\beta_n(X_1)$ also consists of self-similar blocks. For the critical 2^∞ attractor the initial memory lasts infinitely without mixing and creates the self-similar temporal structure. That is, there is no loss of memory of the initial conditions and the future is completely predictable for critical 2^∞ attractor. In an earlier work Gade and Amritkar [25, 26] computed time-dependent fractal exponent for the 2^∞ attractor of the logistic map. It was found to be invariant in time implying no loss of memory. For values of f slightly beyond f_∞ the characteristic feature of $\beta_n(X_1)$ is lost and is on the average found to grow with n. This indicates that a small but finite uncertainty in the initial conditions grows very rapidly with time and after some time it becomes almost impossible to predict the phase-trajectory.

3. Characterization of fluctuations of coarse-grained local expansion rates at bifurcations of chaos

The coarse-grained Lyapunov exponent defined by eq. (2) converge to the unique value Λ^∞ as $n \to \infty$. For a given n, Λ_n depends on the initial point X_1 due to sensitive dependence of chaotic orbit on its initial point. Hence the values of $\Lambda_n(X_1)$ for different X_1's are randomly distributed between a maximum and minimum values. For a given n, the probability density for $\Lambda_n(X_1)$ to take a value around Λ is given by

$$P(\Lambda; n) = \langle \delta(\Lambda_n(X_1) - \Lambda) \rangle, \tag{5}$$

where $\delta(u)$ is the delta function of u and $\langle \cdot \rangle$ denotes the long-time average. The probability density function takes the scaling form [19, 27–29]

$$P(\Lambda; n) = \exp[-n\psi(\Lambda)] P(\Lambda^\infty; n) \tag{6}$$

for $n \to \infty$. To describe the fluctuations of the local expansion rates consider the generating function

$$Z_n(q) = \langle \exp[-n(q-1)\Lambda_n(X_1)] \rangle, \quad (-\infty < q < \infty) \tag{7}$$

and the temporal scaling exponent

$$\phi_n(q) = -\left(\frac{1}{n}\right) \ln Z_n(q)$$

and its derivatives

$$\Lambda_n(q) = \mathrm{d}\phi_n(q)/\mathrm{d}q, \tag{8a}$$

$$\sigma_n(q) = -\mathrm{d}\Lambda_n(q)/\mathrm{d}q, \tag{8b}$$

$$\psi(\Lambda) = \phi(q) + (1-q). \tag{8c}$$

$\sigma_n(q)$ is the variance of fluctuations of $\Lambda_n(X_1)$ around $\Lambda_n(q)$. For $q = 1$, $\phi_n(1)$ becomes zero and $\Lambda_n(1) = \Lambda^\infty$. Further $\Lambda_n(\infty) = \Lambda_{n,\min}$ and $\Lambda_n(-\infty) = \Lambda_{n,\max}$. Therefore, $\Lambda_n(q)$ and $\sigma_n(q)$ with $q > 1$ and $q < 1$ can explicitly describe negative and positive large fluctuations of $\Lambda_n(X_1)$ respectively. The functions $\Lambda_n(q)$, $\sigma_n(q)$, and $\psi(\Lambda)$ are called dynamical structure functions. $\sigma_n(q)$ is computed numerically for chaotic attractors of the DVP oscillator. When the forcing amplitude f is varied from a small value the system (1) shows variety of behaviours such as period doubling route to chaos, band-merging, intermittency, sudden widening of chaotic attractor, etc.

First, we consider intermittent dynamics. In the intermittent chaotic region the time series consists of regular laminar motions interrupted by irregular bursts. Pomeau and Manneville classified the intermittent transitions from stable orbit to chaos (or vice versa) into three types, type-I, II and III according to the local Poincaré map. The characteristic relation of type-I intermittency is $\langle l \rangle \propto (p - p_c)^{-0.5}$ and that of type-II and III is $\langle l \rangle \approx (p - p_c)^{-1}$ where p is the control parameter and p_c is the bifiurcation point and $\langle l \rangle$ is the average laminar length [30]. For the intermittent switching between chaotic bands of the logistic map, the mean life time τ in a chaotic band is found to scale as $\tau \propto (p - p_c)^{-0.5}$ [31, 32]. On the other hand, for intermittency dynamics power spectrum has $1/\omega$ dependence while for fully developed chaos it shows $1/\omega^2$ dependence [33]. For noise-induced intermittency $\langle l \rangle$ scale as $\langle l \rangle \propto (p - p_c)^{-2}$ [34].

In the system (1) for f values just above $f_c = 0.177002$ the system exhibits a period-3 attractor. At $f = f_c$ intermittent dynamics is developed. The laminar motion between two successive bursts have different durations which are randomly distributed over the time series. As the control parameter f is decreased the length of the laminar region decreases. Thus, in the intermittency region the chaotic attractor has two types of local structures which produce the laminar motions and chaotic bursts respectively. The two types of local structures have been captured by the dynamical structure functions.

Figure 3a shows the dynamical structure function $\sigma_n(q)$ for $f = 0.176$ (fully developed chaos), far from intermittency. Here $n = 10$ and $N = 2000$. $\sigma_n(q)$ has a sharp peak at $q = q_\alpha = 1.7$. $\Lambda_n(q)$ is found to exhibit a discontinuous transition at $q = q_\alpha$. For a chaotic motion repeated action of stretching and folding of orbits leads to sensitive dependence of initial conditions. In the folding region a small volume element can be contracted and the expansion rates $\Lambda_n(X_1)$ take negative values leading to $\Lambda_{n,\min} < 0$. The probability for $\Lambda_n(X_1)$ to take negative value decreases with increasing n so that Λ^∞ takes a positive value. However, the dynamical structure functions contains fluctuations of $\Lambda_n(X_1)$ around Λ^∞ including negative values. These negative values give dominant contributions to the eq. (8b) for $q > q_\alpha$.

Figure 3b shows the result for $f = 0.176999$, in the intermittency region, where we used $n = 10$ and $N = 2000$. $\sigma_n(q)$ has two peaks at $q = q_\alpha = 0.75$ and $q = q_\beta = 2.3$. Discontinuities of $\Lambda_n(q)$ are observed at these two values of q. According to thermodynamic

formalism these can be called 'phase transition' like phenomena. The laminar and turbulent bursts produce large fluctuations of the coarse-grained local expansion rates Λ. The q-phase transitions in $\Lambda_n(q)$ and $\sigma_n(q)$ are brought by these fluctuations. For $q_\beta < q < q_\alpha$ the phase is dominated by the orbits with the mean expansion rates $\Lambda = \Lambda^\infty$. As q increases above q_α a q_α-phase transition occurs from the normal phase to a new phase which is dominated by the orbits with $\Lambda \approx \Lambda_{\min} < 0$ representing laminar motion. On the other hand, as q decreases below q_β a q_β-transition occurs from the normal phase to new phase which is dominated by the chaotic orbits with $\Lambda \approx \Lambda_{\max}$.

Next, we consider the band-merging crisis which occurs at $f_c = 0.110650$. For f values just below f_c the chaotic attractor in the Poincaré map consists of two bands. The size of the bands increases with increase in the control parameter f. At $f = f_c$ both the bands merges together and form a single band chaotic attractor. Figure 4 shows $\sigma_n(q)$ versus q for four values of f. Two peaks are observed just before ($f = 0.110644$) (figure 4b) and just after the band-merging ($f = 0.110655$) (figure 4c). Far before ($f = 0.1103$) (figure 4a) and far after the bifurcation ($f = 0.1109$) (figure 4d) single peak alone found.

Finally, we consider the sudden widening of a chaotic attractor. The size of the chaotic attractor which exist for f values slightly below $f < f_c = 0.1855170$ undergoes a sudden increase in size at $f = f_c$. $\sigma_n(q)$ has been computed far before and just before the bifurcation. At $f = 0.1845$ far before the crisis $\sigma_n(q)$ has a single peak while at $f = 0.185488$ (just before the crisis) two peaks were observed. From the above, we note that $\sigma_n(q)$ exhibit a single peak for attractors far from bifurcations and additional peaks in the neighbourhood of the bifurcations.

4. Fluctuation dynamics of coarse-grained state variables

In the previous section we studied fluctuation dynamics of short-time average of local expansion rate. In this section we investigate the fluctuations of short-time average of the state variable x at various bifurcations.

We define the coarse-grained coordinate $\xi_n(X_1)$ as

$$\xi_n(X_1) = \frac{1}{n}\sum_{i=1}^{n} x_i, \tag{9}$$

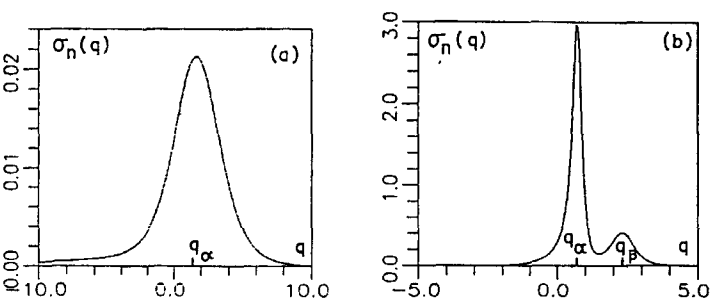

Figure 3. Dynamical structure function $\sigma_n(q)$ for (**a**) far from the intermittent chaos, where $f = 0.176$ and (**b**) in the intermittent chaos region where $f = 0.176999$ with $n = 10$ and $N = 2000$.

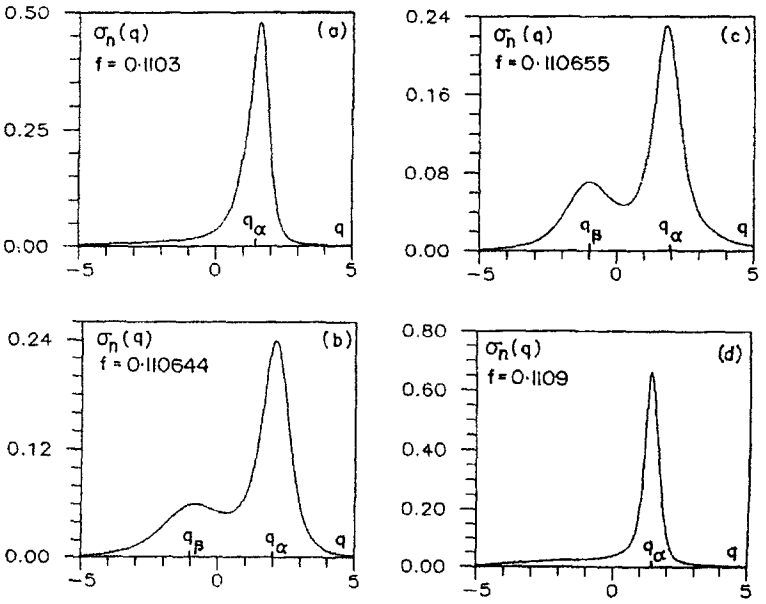

Figure 4. $\sigma_n(q)$ versus q for **(a)** $f = 0.1103$, far before the band-merging, **(b)** $f = 0.110644$, just before the band-merging, **(c)** $f = 0.110655$, just after the band-merging, **(d)** $f = 0.1109$, far after the band-merging.

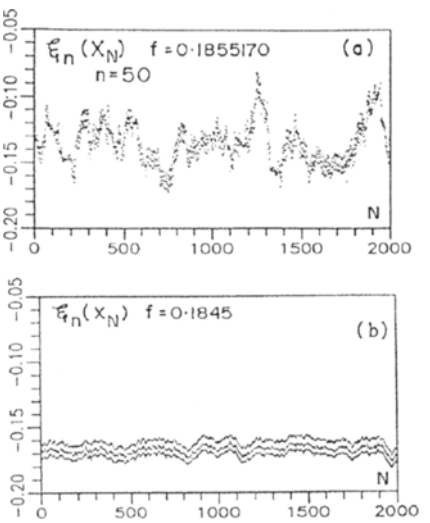

Figure 5. $\xi_n(X_N)$ versus N for the time series of the DVP chaotic attractor system for two values of f.

where x_i are x-component of the system (1) in the Poincaré map and n is finite but large. The limit $n \to \infty$ gives the average value $\xi_\infty = \overline{x}$ whose behaviour will be studied in §6. ξ_∞ is generally independent of the initial condition X_1. However for finite n, ξ_n depends

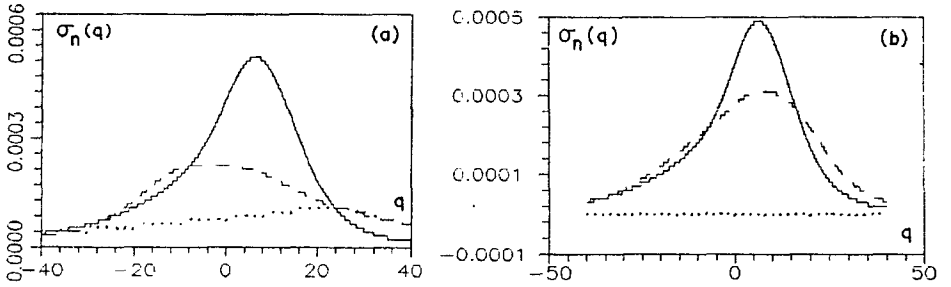

Figure 6. $\sigma_n(q)$ versus q for f values before (a) and after (b) band-merging crisis. The values of f are: **(a)** $f = 0.1103$ far before the band-merging bifurcation (dotted curve), $f = 0.110600$ just before the bifurcation (dashed curve) and $f = 0.110650$ at the bifurcation (continuous curve). **(b)** $f = 0.1110$ far after the band-merging bifurcation (dotted curve), $f = 0.110655$ just after the bifurcation (dashed curve) and $f = 0.110650$ at the bifurcation (continuous curve).

on the initial point X_1. This generates fluctuations of ξ_n. Hence the values of $\xi_n(X_1)$ for different X_1's are randomly distributed between maximum and minimum values.

Far before and far after the critical bifurcations $\xi_n(X_N), N = 1, 2, ...$ are found to be almost constant. However, enormous fluctuations of ξ_n is observed for the parameter values close to the bifurcation values. For example, figure 5 shows $\xi_n(X_N)$ versus N for two values of f. We fixed the value of n at 50. The figure obtained at the sudden widening crisis point $f = f_c = 0.1855170$ (figure 5a) can be compared with the one obtained at $f = 0.1845$ (figure 5b), far before f_c. Large fluctuations of ξ_n appears in the form of bursts in the figure 5a which are absent in figure 5b. We have numerically calculated probability distribution of ξ_n for f values at f_c and far before f_c. Wide distribution is found at the bifurcation value, which is an indication of enormous fluctuations of ξ_n.

In §3 we studied fluctuations of coarse-grained local expansion rate using the quantity $\sigma_n(q)$, eq. (8). The enormous fluctuations of ξ_n occurring in the neighbourhood of bifurcation points can also be characterized in terms of $\sigma_n(q)$ – the variance of fluctuations of $\xi_n(X_1)$ around $\xi_n(q)$. In eq. (7) $\Lambda_n(X_1)$ is replaced by $\xi_n(X_1)$ (eq. (9)). Then the function $\sigma_n(q)$ is calculated for chaotic attractors far away and near the bifurcation values.

First we consider the band-merging bifurcation which occurs in (1) at $f = f_c = 0.110650$. Figure 6a depicts $\sigma_n(q)$ for three values of f. We fixed $n = 75$ in eq. (9) and calculated $Z_n(q)$ by averaging over 8000 values of ξ_n. $\sigma_n(q)$ is flat for far before bifurcation value which implies no fluctuation of ξ_n. However, as f approaches f_c the height of the peak in the $\sigma_n(q)$ versus q plot increases and reaches a maximum value at $f = f_c$. Figure 6b shows the behaviour of $\sigma_n(q)$ after the band-merging. The height of the peak decreases as f is moved away from f_c and becomes flat at $f = 0.1110$. We computed $\sigma_n(q)$ for far away and near the sudden widening and intermittency bifurcations. Here also the height of the peak of $\sigma_n(q)$ increases as the parameter f approach the bifurcation values. Thus $\sigma_n(q)$ is useful for identifying bifurcation points. However, the type of bifurcation cannot be identified from $\sigma_n(q)$.

5. Statistical dynamics of local Lyapunov exponent $\Lambda(X, L)$ and $\bar{x}(L)$

In this section we investigate the variation of local Lyapunov exponent $\Lambda(X_i, L)$ and the quantity $\bar{x}(L)$, the mean value of the variable x, calculated after L time steps in the DVP eq. (1) near bifurcations of chaos. For the system (1) the local Lyapunov exponent $\Lambda(X_i, L)$ is given by eq. (2) with $n = L$. The mean Lyapunov exponent $\bar{\lambda}(L)$ is given by

$$\bar{\lambda}(L) = \lim_{N\to\infty} \frac{1}{N} \sum_{i=1}^{N} \Lambda(X_i, L). \tag{10}$$

The local Lyapunov exponent is relevant when one wants to know the predictability of a system either locally in the phase space of the attractor or by the variation of the average exponent over the attractor. We consider the variance of Λ about $\bar{\lambda}(L)$ which is given by

$$\sigma_\Lambda^2(L) = \lim_{N\to\infty} \frac{1}{N} \sum_{i=1}^{N} [\Lambda(X_i, L) - \bar{\lambda}(L)]^2. \tag{11}$$

Its square root is the standard deviation. Similar to the mean Lyapunov exponent we define

$$\bar{x}(L) = \lim_{N\to\infty} \frac{1}{N} \sum_{i=1}^{N} \xi(X_i, L), \tag{12}$$

where $\xi(X_i, L)$ is given by eq. (9) with $n = L$. We study the behaviour of σ_Λ and σ_ξ near the critical bifurcations.

In the calculations of Λ and ξ we have limited to the following values of L: $2^i, i = 2, 3, ..., 11$. Figure 7 shows the plot of σ_Λ versus L in $\log_2 - \log_2$ scale for four values of f near the sudden widening crisis ($f_c = 0.1855170$). The numerically computed data points fall nicely on straight lines in $\log_2 - \log_2$ scale implying power-law dependence of σ_Λ on

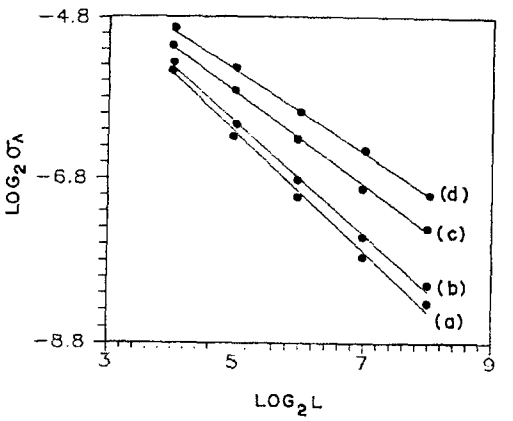

Figure 7. σ_Λ versus L in $\log_2 - \log_2$ scale for various values of f near sudden widening bifurcation in the DVP system. The values of f are: (a) 0.185488, (b) 0.1854895, (c) 0.1855105 and (d) 0.1855177. For these four values of f, σ_Λ is found to scale $0.166L^{-0.729}$, $0.157L^{-0.688}$, $0.134L^{-0.569}$ and $0.131L^{-0.508}$ respectively.

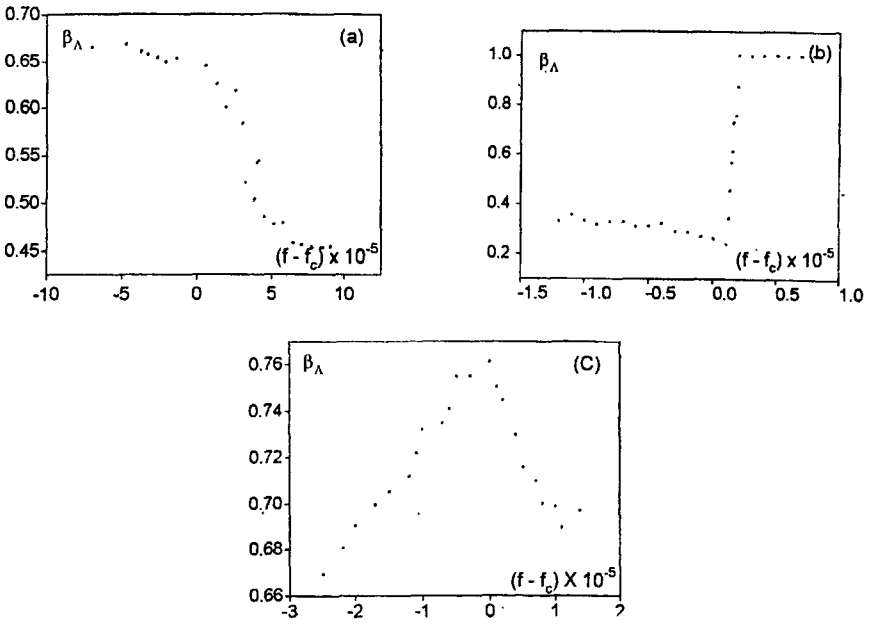

Figure 8. Variation of β_Λ near the sudden widening (**a**), intermittency (**b**) and band-merging (**c**) bifurcations.

L. σ_ξ is also found to show power-law variation. That is, σ_Λ and σ_ξ approach zero in the limit $L \to \infty$ as $L^{-\beta}$. β_Λ is found to be 0.5 [35] based on a central limit theorem kind of assumption while 1 [36] based on analyticity in time. From figure 7, it is evident that slopes of the best straight line fit to the data obtained for various values of f are different. That is, the exponent β_Λ depends on the control parameter f.

Figure 8a–c depict the variation of β_Λ near the sudden widening, intermittency and band-merging bifurcations. Abrupt variation of β_Λ and β_ξ (not shown) are found near the sudden widening and intermittency bifurcations. Linear variation of β_Λ and β_ξ with different rate is observed just before and just after the band-merging bifurcation.

6. Variation of mean value of state variable and Lyapunov exponent

The mean value of the state variable x is given by

$$\bar{x} = \lim_{N\to\infty} \frac{1}{N} \sum_{i=1}^{N} x_i, \tag{13}$$

where x_i is the x-component of the ith Poincaré point. In the system (1), as mentioned earlier intermittent chaos is observed when the parameter f is decreased from $f_c = 0.177002$. Figure 9a shows the variation of $\bar{x}$ near f_c where dots represent numerical data with $N = 10^4$ and the continuous line is the power-law fit to the numerical data. In this figure $\bar{x}$ is almost constant for values of f just above f_c. However,

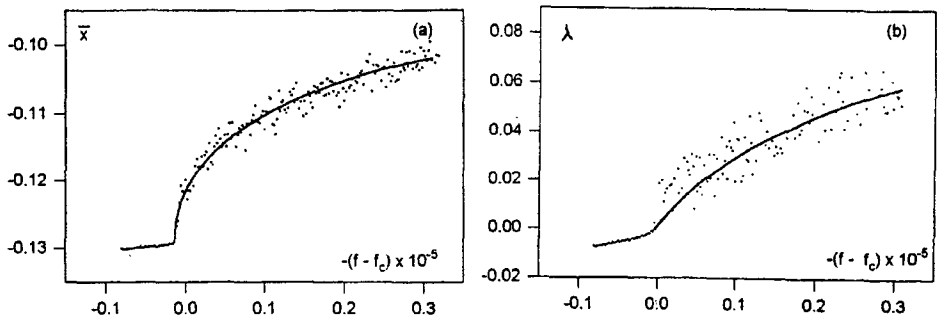

Figure 9. Variation of mean value $\bar{x}$ **(a)** and Lyapunov exponent **(b)** of the DVP oscillator equation near intermittent crisis. Dots are numerical data and continuous line is the best power-law fit to the data.

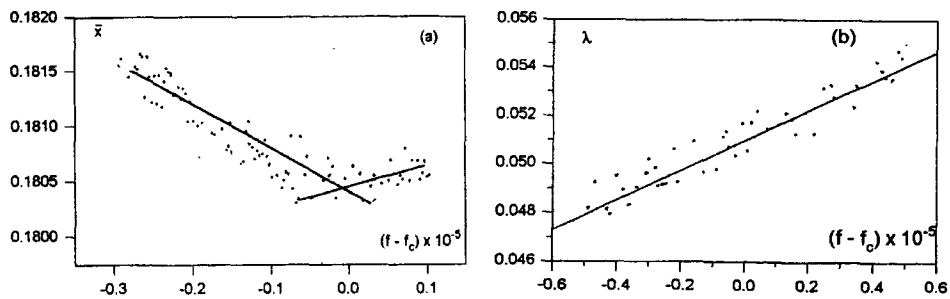

Figure 10. Dependendence of $\bar{x}$ **(a)** and λ **(b)** near band-merging bifurcation in the DVP equation.

abrupt variation is clearly seen just after the bifurcation value f_c. $\bar{x}$ is found to vary as $\bar{x} \approx -0.0976 \mid f - f_c \mid^{-0.0475}$ where $\mid f - f_c \mid$ is in units of 10^{-5}. For sudden widening we found $\bar{x} \approx -0.1440 \mid f - f_c \mid^{0.0206}$. Power-law variation of maximal Lyapunov exponent λ is found for both intermittency (figure 9b) and sudden widening crises. λ is found to vary as $\lambda \approx 0.0634 \mid f - f_c \mid^{0.3189}$ in the intermittency region and $\lambda \approx 0.0764 \mid f - f_c \mid^{0.0235}$ just after sudden widening crisis. The abrupt variation of $\bar{x}$ and λ corresponds to an increase in the size of the attractor.

Next, we consider band-merging crisis occurring at $f = f_c = 0.110650$. From just before and as well as just after the bifurcation the size of the attractor increase linearly with the control parameter. Consequently, one may expect linear variation of $\bar{x}$ and λ near the bifurcation. Figure 10a shows the behaviour of $\bar{x}$ near band-merging. In this figure we see that the rate of variation of $\bar{x}$ (slope of the straight line fit) is different for $f < f_c$ and $f > f_c$. The curve has a sharp knee at $f = f_c$. For $f < f_c$ we obtained the relation $\bar{x} \approx 0.1804 - 0.00278(f - f_c)$, while for $f > f_c$: $\bar{x} \approx 0.1804 - 0.00281(f - f_c)$. Linear variation of λ is observed near the band-merging (figure 10b where for $f < f_c : \lambda \approx 0.05097 + 0.00615(f - f_c)$ and $f > f_c : \lambda \approx 0.05097 + 0.00615(f - f_c)$.

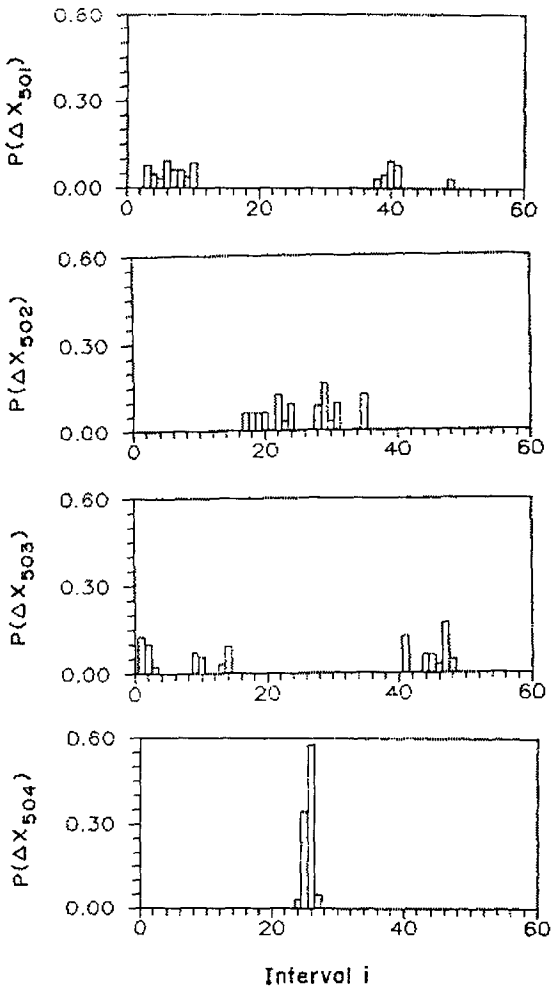

Figure 11. Numerically calculated $P(\Delta x_k)$, $k = 501, 502, 503, 504$ for $f = 0.10976680$. P is nonstationary.

7. Characterization of weak and strong chaos

It is well known that the essential characteristic of chaotic motion is its sensitive dependence on initial conditions which leads to unpredictability of the long time evolution of chaotic systems. This is characterized by the positive Lyapunov exponent. In nonlinear dynamics literature chaotic dynamics with positive but very small maximal Lyapunov exponent is termed as weak chaos while the chaotic dynamics with positive and relatively large maximal Lyapunov exponent is called strong chaos. In this section we focus our study on the characterization of weak and strong chaos in the DVP eq. (1). Let us consider the probability distribution $P(\Delta x_k), k = 1, 2, ...$ of the k-step difference quantity

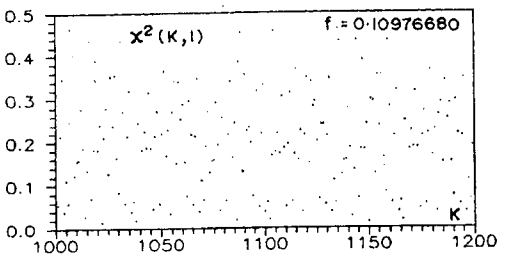

Figure 12. $\chi^2(k,1)$ versus k for $f = 0.10976680$. P is nonstationary.

$$\Delta x_k = x_{m+k} - x_m, \tag{14}$$

where $m = 1, 2, ..., N', N' < N - k$. We calculated the probability distribution of $\{\Delta x_k\}$ as follows. The maximum and minimum values of $\{\Delta x_k\}$ are determined. The range of Δx_k is divided into a finite number (M) of equal interval. We then counted the number of occurrences of Δx_k in each interval and obtained the probability distribution $P(\Delta x_k)$ (hereafter called as P) by dividing the numbers by the total number.

The maximal Lyapunov exponent λ is numerically computed as a function of f in the interval $(0.10, 0.115)$. There are many regions in which λ is positive but very small indicating weak chaos. For example, for $f = 0.10976680$ a chaotic attractor with $\lambda = 0.0005$ is found. Figure (11) shows the evolution of P for $k = 501, 502, 503, 504$. P is changing with k. That is, the distribution is nonstationary. This is further verified by the chi-square, χ^2, test. The test quantity is defined as [37]

$$\chi^2(k;j) = \sum_{i=1}^{M} \frac{(R_i - S_i)^2}{(R_i + S_i)}, \tag{15}$$

where R_i and S_i are the probabilities of the ith interval for $P(\Delta x_{k+j})$ and $P(\Delta x_k)$ respectively. In the eq. (15) interval with $R_i = S_i = 0$ are excluded. If two probabilities differ very much we get a large χ^2. For two similar distributions χ^2 will be small. The numerically calculated χ^2 is plotted in figure 12. The nondecreasing χ^2 implies the nonstationary characteristics of P. The occurrence of a nonstationary probability distribution implies that a complete probability distribution is impossible.

A possible mechanism of nonstationary probability distribution can be a recurrence of memory loss and recovery of initial conditions [25, 26]. The key to searching for memory recovery is the value of the Lyapunov exponent. Chern and Otsuka [38] applied information theory and a local Lyapunov exponent to characterize the locally deforming nature in chaos. Particularly, using self-information and mutual information flows they have shown that memory recovery is possible for chaos with a very small positive Lyapunov exponent. Thus the physical mechanism of the nonstationary probability distribution is the recurrence of memory loss and the recovery of initial conditions.

Stationary probability distribution is found for strong chaos. We consider a two-band chaotic attractor. A two-band chaotic attractor is found to occur for $f = 0.1105$. Its maximal Lyapunov exponent is $(\lambda = 0.0436)$. Figure 13 shows P for $k = 501, 502, 503, 504$. A simple switching between two classes of probability distribution can be clearly seen. This is because x_n keeps on alternating between the two bands of the chaotic attractor.

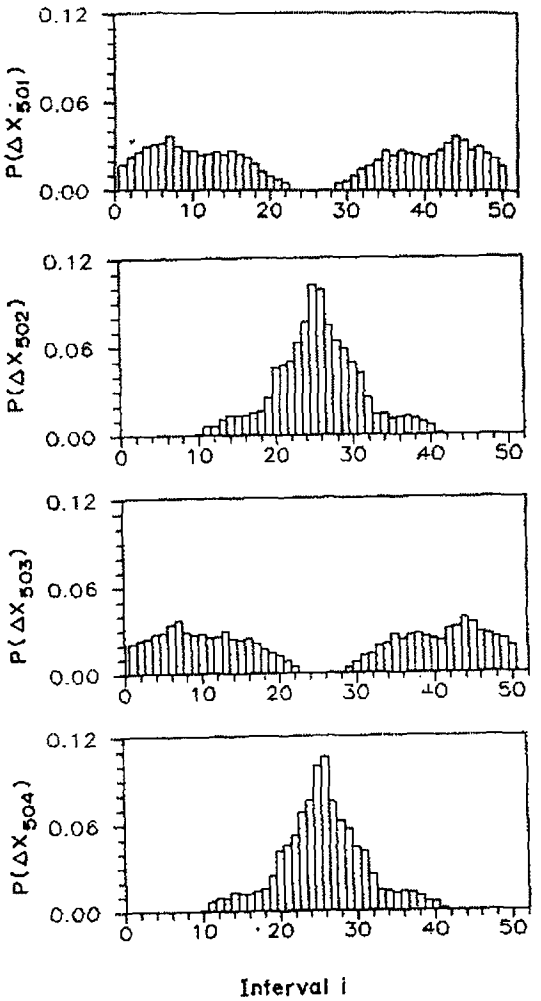

Figure 13. Evolution of P for a two-band chaotic attractor . The value of f is 0.1105.

$\chi^2(k,1)$ and $\chi^2(k,2)$ are calculated. $\chi^2(k,1)$ is found to be large while $\chi^2(k,2)$ is found to decay to zero with increase in k. The distribution is stationary. As an another example for stationary probability P we consider the single band chaos at $f = 0.1108\,(\lambda = 0.0566)$. After $k = 25$, χ^2 (figure 14) becomes ≈ 0. That is, the distribution has evolved into a stationary state. This suggest that the variable x_n can be described as if it were generated by a random number generator with a certain probability distribution. A possible mechanism for stationary probability distribution is a complete loss of memory to the initial condition [17, 18]. The above study suggests that the analysis of probability distribution characteristics of chaos can be used to distinguish weak and strong chaos.

Nonstationary P occurs for a range of values of the control parameter f for which maximal Lyapunov exponent is relatively small. We have investigated the dependence of the degree of nonstationarity of P with the control parameter and Lyapunov exponent. For this

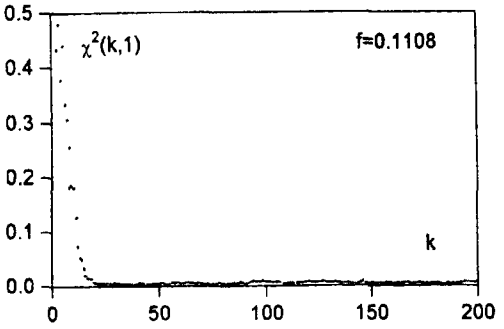

Figure 14. Numerically calculated $\chi^2(k,1)$ at $f = 0.1108$ (strong chaos).

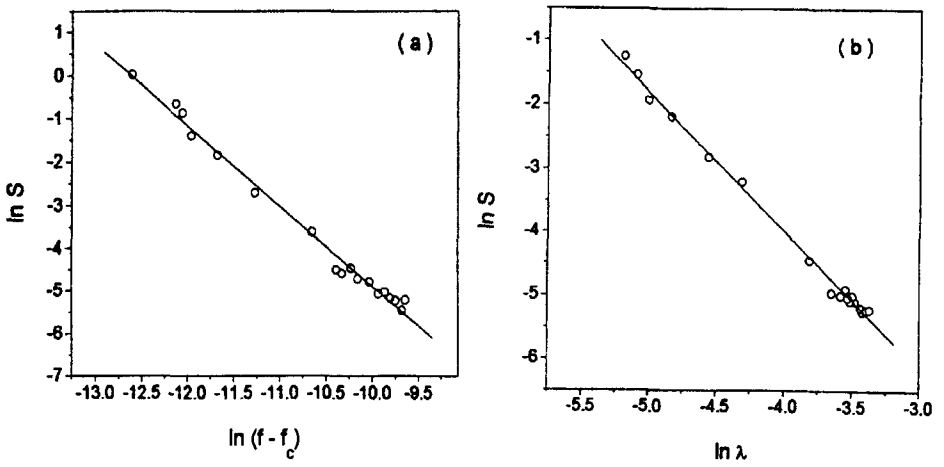

Figure 15. (a) S versus $(f - f_c)$ and (b) S versus λ in the ln–ln scale where $f_c = 0.110250$. We found $S \propto (f - f_c)^{-\alpha}$ where $\alpha = 1.87$ and $S \propto \lambda^{-\alpha}$ where $\alpha = 2.17$.

purpose, we define the quantity S, the degree of nonstationarity of $P(\Delta x_k)$, as

$$S = \lim_{N\to\infty} \frac{1}{N} \sum_{k=1}^{N} \chi^2(k;j), \tag{16}$$

where $\chi^2(k;j)$ is given by eq. (15). For strong chaos $\chi^2 \to 0$ for large k and hence $S = 0$. Since χ^2 does not decay to zero for weak chaos in the limit $k \to \infty$ evidently S is non-zero. The magnitude of S characterizes the degree of different nonstationary probability distributions. S is calculated for a range of values of f in the DVP oscillator. Figure 15a shows S versus $(f - f_c)$ in the ln–ln scale. Circles represent the numerical data and continuous line is the best straight line fit. Here f_c refers to the f value at which $\lambda \approx 0$ and above (or below) which chaos occurs. Power-law variation of S with $(f - f_c)$ is observed. S is found to approach zero as $(f - f_c)^{-\alpha}$, where α is a constant and is calculated as 1.87. Figure 15b depicts S versus λ. We note that as λ increases S decays to zero. That is transition from nonstationary P to stationary P occurs as λ increases from zero and we found $S \propto \lambda^{-\alpha}$ where $\alpha = 2.17$.

8. Summary and conclusion

In this paper we have studied the characteristic features associated with the variation of certain statistical quantities at critical bifurcations of chaos in DVP oscillator eq. (1). The variance of local expansion rate exhibits self-similar pattern at the onset of chaos where $\lambda \approx 0$. We have shown that the variations of $\Lambda(X, L)$ and $\xi(X, L)$ about their mean values approach zero in the limit $L \to \infty$. This approach is as $L^{-\beta}$. The exponent β is found to show abrupt variation near the critical bifurcations.

In the neighbourhood of critical bifurcations enormous fluctuations of the coarse-grained local expansion rate and coordinate ξ_n is observed. The fluctuation dynamics is studied using the variance $\sigma_n(q)$. $\sigma_n(q)$ associated with the local expansion rate and the coordinate ξ_n show different characteristic features. When the local expansion rate is considered $\sigma_n(q)$ versus q plot exhibits a peak at $q = q_\alpha$ for all chaotic attractors of the DVP eq. (1). However, additional peaks are found near the critical bifurcation only. On the other hand, when the fluctuations of the coarse-grained coordinate ξ_n is considered we observed flat $\sigma_n(q)$ spectrum far before and far after the bifurcations. When the values of the control parameter approaches the critical bifurcation values from far before and as well as from far after the bifurcation, the height of the peak in the $\sigma_n(q)$ versus q plot increase and reach the maximum value at the critical values. Even though it is not clear how to distinguish different bifurcations using $\sigma_n(q)$, it is useful to identify the parametric values at which bifurcation of chaos occur.

The average values of the state variable $\bar{x}$ and the maximal Lyapunov exponent λ are found to vary abruptly near bifurcation values. In the sudden widening and intermittency bifurcations power-law variation of $\bar{x}$ and λ is observed only on one side of the critical value. This is because in both the bifurcations the size of the attractor is suddenly increased at the bifurcations. In contrast to this, in the band-merging bifurcation the size of the attractor increases linearly with the control parameter and consequently $\bar{x}$ and λ show linear variation on either side of the bifurcation point. Finally, we have shown that the probability distribution $P(\Delta x_k)$ can be used to identify weak and strong chaos.

Acknowledgement

The work of (SR) forms part of a Department of Science and Technology, Government of India sponsored research project. Part of the numerical computation was done at the Centre for Nonlinear Dynamics, Bharathidasan University, Thiruchirapalli. The authors thank the referee for critical comments and suggestions which improved the presentation of this paper.

References

[1] H G Schüster, *Deterministic chaos* (Verlag Chemie, Weinheim, 1988)
[2] M Lakshmanan and K Murali, *Chaos in nonlinear oscillators* (World Scientific, Singapore, 1996)
[3] J K Bhattacharjee, *Convection and chaos in fluids* (World Scientific, Singapore, 1987)
[4] E Ott, *Chaos in dynamical systems* (Cambridge University Press, Cambridge, 1993)
[5] S Neil Rasband, *Chaotic dynamics of nonlinear systems* (John-Wiley, New York, 1990)

[6] B Huberman and J Rudnick, *Phys. Rev. Lett.* **45**, 154 (1980)
[7] S C Johnston and R C Hilborn, *Phys. Rev.* **A37**, 2680 (1988)
[8] Y C Lai, *Phys. Rev.* **E53**, 57 (1996)
[9] V Mehra and R Ramaswamy, *Phys. Rev.* **E53**, 3420 (1996)
[10] A Prasad, V Mehra and R Ramaswamy, *Phys. Rev.* **E57**, 1576 (1998)
[11] N Voglis and G J Contopoulos, *J. Phys.* **A27**, 4899 (1994)
[12] H D I Abarbanel, R Brown and M B Kennel, *J. Nonlinear Sci.* **1**, 175 (1991)
[13] C Amitrano and R S Berry, *Phys. Rev.* **E47**, 3158 (1993)
[14] A Prasad, V Mehra and R Ramaswamy, *Phys. Rev. Lett.* **79**, 4127 (1997)
[15] S Rajasekar, S Parthasarathy and M Lakshmanan, *Chaos, Solitons and Fractals* **2**, 271 (1992)
[16] J Fang, *Phys. Lett.* **A146**, 35 (1990)
[17] G P King and S T Gaito, *Phys. Rev.* **A46**, 3092 (1992)
[18] M G M Gomes and G P King, *Phys. Rev.* **A46**, 3100 (1992)
[19] H Shibata, S Kuroki and H Mori, *Prog. Theor. Phys.* **83**, 829 (1990)
[20] A Wolf, J B Swift, H L Swinney and J A Vastano, *Physica* **D16**, 285 (1985)
[21] S Rajasekar and M Lakshmanan, *Physica* **D67**, 282 (1993)
[22] S Rajasekar and M Lakshmanan, *J. Theor. Bilo.* **166**, 275 (1994)
[23] S Rajasekar, *Pramana – J. Phys.* **39**, 509 (1992)
[24] S Rajasekar and P Muruganandam (unpublished)
[25] P M Gade and R E Amritkar, *Phys. Rev. Lett.* **65**, 389 (1990)
[26] P M Gade and R E Amritkar, *Phys. Rev.* **A45**, 725 (1992)
[27] H Fujisaka and M Inoue, *Prog. Theor. Phys.* **77**, 1334 (1987)
[28] H Shibata, H Fujisaka and H Mori, *Physica* **A189**, 554 (1992)
[29] R Ishizaki, T Horita and H Mori, *Prog. Theor. Phys.* **89**, 947 (1993)
[30] Y Pomeau and P Manneville, *Commun. Math. Phys.* **74**, 189 (1980)
[31] C Grebogi, E Ott, F Romeiras and J A Yorke, *Phys. Rev.* **A36**, 5365 (1987)
[32] H Shibata, S Kurokiand and H Mori, *Prog. Theor. Phys.* **83**, 829 (1990)
[33] E G Gwinn and R M Westervelt, *Phys. Rev.* **A33**, 4143 (1986)
[34] T C Halsey, M H Jenson, L P Kadanoff, I Procaccia and B Shraiman, *Phys. Rev.* **A33**, 1141 (1986)
[35] P Grassberger, R Badii and A Politi, *J. Stat. Phys.* **51**, 135 (1988)
[36] I Goldhirsch, P L Sulem and S A Orzag, *Physica* **D27**, 311 (1986)
[37] J L Chern and T C Chow, *Phys. Lett.* **A192**, 34 (1994)
[38] J L Chern and K Otsuka, *Phys. Lett.* **A188**, 321 (1994)